The Role of Backbone Flexibility in the Accommodation of Variants That Repack the Core of T4 Lysozyme

E. P. Baldwin, O. Hajiseyedjavadi, W. A. Baase, B. W. Matthews*

To understand better how the packing of side chains within the core influences protein structure and stability, the crystal structures were determined for eight variants of T4 lysozyme, each of which contains three to five substitutions at adjacent interior sites. Concerted main-chain and side-chain displacements, with movements of helical segments as large as 0.8 angstrom, were observed. In contrast, the angular conformations of the mutated side chains tended to remain unchanged, with torsion angles within 20° of those in the wild-type structure. These observations suggest that not only the rotation of side chains but also movements of the main chain must be considered in the evaluation of which amino acid sequences are compatible with a given protein fold.

Water-soluble proteins fold into compact structures that generally have hydrophobic side chains in the interior and polar residues on the exterior, suggesting that patterns of hydrophobicity in amino acid sequences are important determinants of protein structure (*1*). Mutations that reduce the hydrophobicity of buried residues are often destabilizing (*2*, *3*). However, the contribution of specific interactions between buried hydrophobic side chains to protein structure and stability is less clear. Side chains in protein interiors or "cores" are tightly packed (*4*) and usually adopt single, well-defined, low-energy conformations (*5*). That core residues maximize favorable interactions with minimum strain suggests that a particular protein fold may be specified by a "template" of packed hydrophobic side chains (*6*). In support of this idea, the computational enumeration and evaluation of all the possible combinations of side chains that can fill a given volume in the core of known protein structures yielded few allowed sequences (*6*). However, genetic experiments by Sauer and co-workers demonstrated that λ repressor tolerated multiple substitutions within the interior (*7*, *8*). Many variants with different combinations of interior hydrophobic side chains were functional, and a significant fraction were only moderately destabilized (*8*). This result poses two questions: (i) How are the different side chains arranged in the interior, and (ii) how has the rest of the protein adjusted? To address these questions, we obtained T4 lysozyme variants with altered hydrophobic cores and determined their three-dimensional structures.

The largest contiguous hydrophobic core in T4 lysozyme resides in the COOH-terminal domain (residues 81 to 164). Five adjacent buried residues in this region were targeted for substitution: Leu^{121}, Ala^{129}, Leu^{133}, Val^{149}, and Phe^{153} (Fig. 1A). The variants were generated by site-specific random mutagenesis and genetic selection of the resulting mutant pool for enzyme function (*9*). High-resolution structures and folding energies (*10*) of eight variants containing three to five substitutions were determined (Table 1).

All variants were less stable than the wt protein (−1.1 to −3.5 kcal/mol) but not by more than expected for a single interior substitution (*3*, *11*). Differences in stabilities relative to wild type do not directly correspond to changes in total side chain transfer energies (−2.2 to +2.7 kcal/mol for octanol to water) (*12*) or van der Waals volumes (−85 to +102 Å^3, equivalent to −5 to +6 methylene volumes) (*4*), although the less stable proteins are those with smaller and less hydrophobic cores (Table 1). Lysozyme mutants containing the individual substitutions that comprise the multiple variants were also constructed, and their stabilities were determined. The sum of the ΔΔG values for the singly

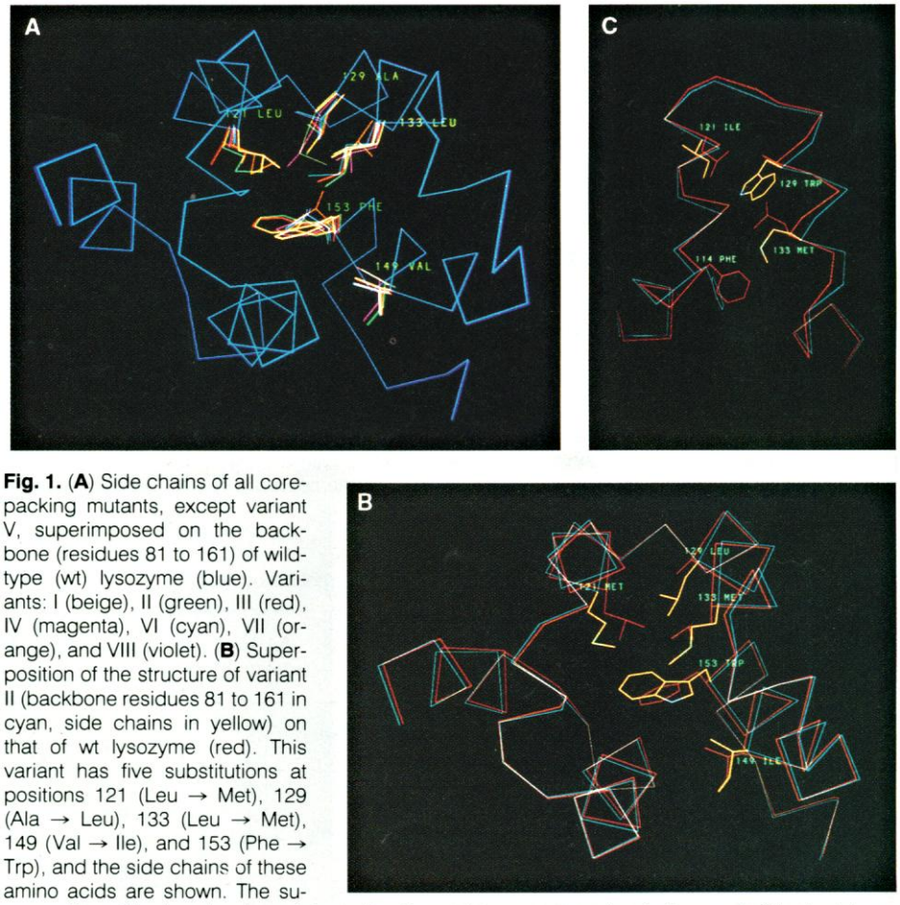

Fig. 1. (**A**) Side chains of all core-packing mutants, except variant V, superimposed on the backbone (residues 81 to 161) of wild-type (wt) lysozyme (blue). Variants: I (beige), II (green), III (red), IV (magenta), VI (cyan), VII (orange), and VIII (violet). (**B**) Superposition of the structure of variant II (backbone residues 81 to 161 in cyan, side chains in yellow) on that of wt lysozyme (red). This variant has five substitutions at positions 121 (Leu → Met), 129 (Ala → Leu), 133 (Leu → Met), 149 (Val → Ile), and 153 (Phe → Trp), and the side chains of these amino acids are shown. The superposition of the two structures is based on the root-mean-square (rms) alignment of the backbone atoms within the COOH-terminal domains. The labels identify the altered amino acids. (**C**) Superposition of the structure of variant V (backbone residues 106 to 141 in cyan, side chains in yellow) on that of wt lysozyme (red). This variant has three substitutions, 121 (Leu → Ile), 129 (Ala → Trp), and 133 (Leu → Met). Also shown is the side chain of Phe^{114}, which underwent a substantial rotation.

Institute of Molecular Biology, Howard Hughes Medical Institute, and Department of Physics, University of Oregon, Eugene, OR 97403.

*To whom correspondence should be addressed.

substituted mutants exceeded the ΔΔG value observed for the corresponding multiply substituted mutant by up to 3.9 kcal/mol. This difference indicates that the individual substitutions interact favorably (*11, 13*).

As observed for λ repressor (*7, 8*), the structure and activity of T4 lysozyme are tolerant to a variety of combinations of hydrophobic residues in the core. However, the patterns of substitutions observed at each site differ. The examples shown in Table 1 reflect the variation in a larger set of 106 selected variants (9). Sites 121 and 129 allow a wide variety of hydrophobic residues, but at position 149 Val or Ile residues seem to be required for stability (*14*).

In seven of the eight variants, each replacement side chain occupied the same region of the core as the corresponding side chain in the wt protein (Fig. 1A). A representative of this group, variant II, is shown in Fig. 1B. The amino acids present in the mutant differ from wild type at all five positions, but the destabilization is modest (1.3 kcal/mol). The remaining mutant (variant V) has the largest overall structural changes. It includes the potentially disruptive substitution Ala^{129} to Trp and has one of the largest increases in side chain volume (Table 1). In this case, some of the side chains move substantially relative to their positions in the wt structure (Fig. 1C). For all mutants, the replacement side chains are accommodated by a combination of backbone adjustments and side-chain displacements. Because of the lever arm involved, a shift of 1 to 2 Å in the distal atoms of a side chain can be accompanied by smaller changes (~0.5 Å) in the backbone. In variant II (Fig. 1B), for example, Met^{121} has side chain torsion angles nearly identical to those of Leu^{121} in wild type, but the δ atoms are displaced by 1.7 Å. The α-carbon atom moves only 0.6 Å.

Root-mean-square (rms) shifts in backbone atoms for the eight variants range from 0.17 to 0.63 Å (Table 1 and Fig. 2) (*15*). Helices move up to 0.8 Å (Fig. 2) by a combination of rotations and translations (*16*) with individual α-carbon atoms moving up to 1.7 Å. The largest backbone adjustments occur in the variants having the largest increases in core volume. These adjustments correspond to an overall expansion of the COOH-terminal domain (compare the mutant backbone in Fig. 1, B and C, with that of wild type).

Although the replacement side chains have adjusted their positions (Fig. 1, A to C), their torsion angles are within 20° of those of the wild type, with the exception of position 153 (Fig. 3). In other words, the mutant side chains usually retain the same rotational conformation present in wild type (*17*). Change in conformation of even a single side chain may be difficult to accommodate because it may require conformational changes in surrounding side chains. In one lysozyme variant that did display several side chain rotations (variant V, Fig. 1C), the small-to-large substitution of Ala^{129} to Trp introduced a potential steric clash with Met^{133}, which is within the same α helix. As a result, Met^{133} adopted a side chain conformation not seen in other variants containing Met at this position (*18*). Coupled with this change in conformation, the benzyl group of Phe^{114}, which has access to the surface and therefore is more free to move, rotated 80°. This variant, which has rms backbone shifts of 0.63 Å but is only destabilized by 1.4 kcal/mol, illustrates that large structural adjustments that alter the positions of atoms throughout the COOH-terminal domain need not disrupt favorable interactions between them.

Computational methods have been developed to enumerate alternative combinations of side chains in the context of a particular protein fold (*6, 19–21*). All such approaches have focused on rotational changes of side chains with the position of the backbone held fixed, at least during the critical evaluation process. Given the magnitude of backbone shifts we have observed, it is likely that algorithms that use steric criteria to eliminate side chain combina-

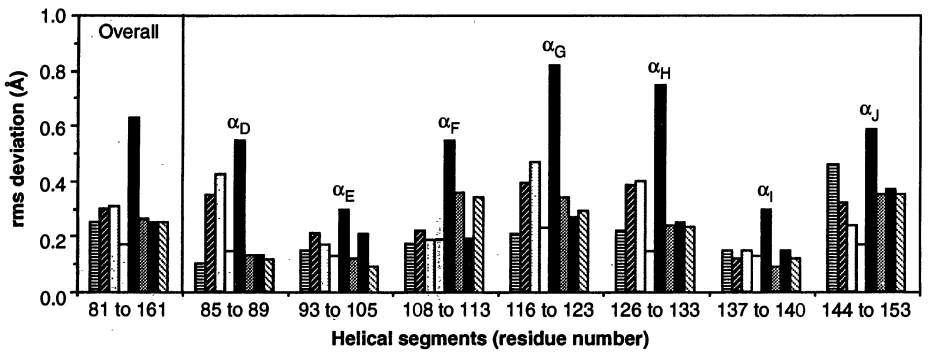

Fig. 2. Shifts in individual helices. For each variant the backbone atoms within the COOH-terminal domain (residues 81 to 161) were superimposed on wild type. The rms differences for the backbone atoms within each of the seven α helices (α_D to α_J) in the COOH-terminal domain are shown. The rms differences for all backbone atoms within the COOH-domain are also shown at the left. The order of the variants corresponds to their relative stabilities as numbered in Table 1, leftmost (variant I) to rightmost (variant VIII).

Table 1. Sequences and properties of core-packing variants, ranked by stability.

Protein	Mutation site					ΔΔG* (kcal/mol)	$\Delta\Delta G_{SOL}$† (kcal/mol)	$\Delta V_{side\ chain}$‡ ($Å^3$)	Resolution§ (Å)	*R*§ (%)	Change in backbone‖ (Å)
	121	129	133	149	153						
Wild type	Leu	Ala	Leu	Val	Phe	—	—	—	1.7	17.0	—
I	Ala	Met	—	—	Leu	−1.1	−0.8	−11	2.1	15.1	0.25
II	Met	Leu	Met	Ile	Trp	−1.3	+2.1	+102	1.85	16.6	0.29
III	Ile	Leu	Met	—	Trp	−1.3	+2.0	+84	2.1	14.9	0.31
IV	Ala	Met	—	Ile	—	−1.4	+0.2	+18	2.0	15.3	0.17
V	Ile	Trp	Met	—	—	−1.4	+2.2	+95	2.0	16.6	0.63
VI	Ala	Val	Met	—	Leu	−2.3	−1.4	−29	2.0	15.8	0.26
VII	Met	—	Val	—	Leu	−2.5	−1.4	−29	2.1	16.6	0.25
VIII	Ala	Val	Ala	—	Leu	−3.5	−2.7	−85	2.0	16.2	0.25

*The difference between the free energy of unfolding of the mutant (*33*) and that of wt protein (ΔΔG) was calculated with a reference temperature of 51.7°C and a change in heat capacity ΔC_p = 2.5 kcal/mol per degree (*3, 11*). The estimated error in ΔΔG increases from 0.2 kcal/mol for mutants with stabilities close to that of the wild type to 0.5 kcal/mol for the least stable variants. †$\Delta\Delta G_{SOL}$ is the difference between the octanol-water transfer energies (*12*) of the side chains in the mutant and those in wild type. ‡The overall changes in the side chain volumes of the substituted residues ($\Delta V_{side\ chain}$) were calculated from the individual side chain volumes (*4*). §The crystallographic residual, *R*, was calculated with the use of all reflections from 10 Å to the limiting resolution (data completeness of 78 to 93%). ‖The change in backbone is as defined in Fig. 2.

tions that clash in the context of a fixed backbone are overly restrictive (*11, 20*). In support of this idea, calculations based on the combination of the wt T4 lysozyme backbone with variant side chains in "standard" conformations (6) indicated that none of the variants in Table 1 were "allowed." If the crystallographically observed backbone was used for a given T4 variant, then the number of "unacceptable" close contacts was greatly reduced. However, most variants were still "not allowed," suggesting that the use of "average" torsion angles is also unsatisfactory. Small departures of torsion angles from average values can lead to large displacements of distal atoms, resulting in an unrealistic assessment of contacts (*11*). Our results do, however, support the idea that side chain conformations in a known protein structure can provide a reasonable starting point in the prediction of the structure of a homologous protein (*21*).

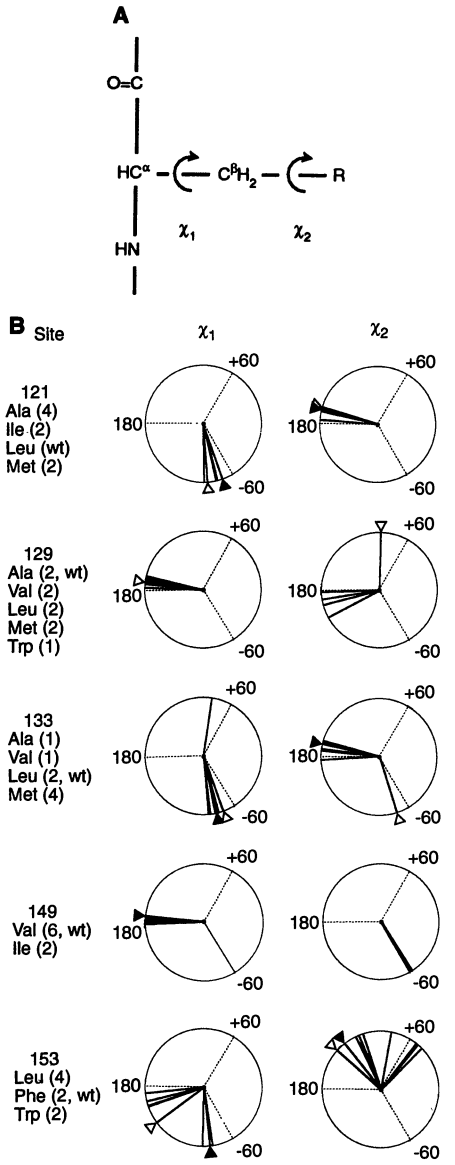

Fig. 3. (**A**) Side chain torsional angles, χ_1 and χ_2. (**B**) Neuman projections of the side-chain torsion angles. The sites of substitution and the different amino acids that occur at each site are given on the left with the number of occurrences in parentheses. The torsion angles in the wt structure are indicated by the solid arrowheads; the torsion angles in variant V, which has the largest structural changes of all mutants, are indicated by the open arrowheads. Torsion angles were calculated according to the definitions of the International Union of Pure and Applied Chemistry (*31*) except for special cases involving branched side chains (*32*).

The structures of T4 lysozyme mutants studied here and elsewhere (*3, 11*), and a variant of λ repressor (*22*), suggest that protein backbones are more flexible than generally assumed. Even a few replacements of interior side chains can cause differences in the backbone structure of magnitude similar to that seen between homologous structures with much less sequence similarity. For proteins whose overall sequence identity is 50% or greater, the differences in backbone are 0.3 to 1.5 Å, whereas the side chain torsion angles tend to be preserved (*21, 23*). Concerted backbone and side chain shifts, along with small alterations in torsion angles, are sufficient to allow alternative side chains to pack without necessarily large destabilization. Structures of the same protein in different crystal-packing environments (*23, 24*) reveal changes in the structure of magnitude similar to those reported here. Therefore, some of the flexibility we observe may be intrinsic to native protein structures rather than induced only by major changes in internal architecture.

REFERENCES AND NOTES

1. J. U. Bowie, R. Lüthy, D. Eisenberg, *Science* **253**, 164 (1991).
2. M. Matsumura *et al.*, *Nature* **334**, 406 (1988); J. T. Kellis, K. Nyberg, D. Sali, A. R. Fersht, *ibid.* **333**, 784 (1988); D. Shortle, W. E. Stites, A. K. Meeker, *Biochemistry* **29**, 8033 (1990).
3. E. A. Eriksson *et al.*, *Science* **255**, 178 (1992); A. E. Eriksson *et al.*, *J. Mol. Biol.* **229**, 747 (1993).
4. F. M. Richards, *J. Mol. Biol.* **82**, 1 (1974).
5. R. Chandrasekaran and G. N. Ramachandran, *Int. J. Protein Res.* **2**, 223 (1970); J. Janin, S. Wodak, M. Levitt, B. Maigret, *J. Mol. Biol.* **125**, 357 (1978).
6. J. W. Ponder and F. M. Richards, *J. Mol. Biol.* **193**, 775 (1987).
7. W. A. Lim and R. T. Sauer, *Nature* **339**, 31 (1989).
8. W. A. Lim, D. C. Farruggio, R. T. Sauer, *Biochemistry* **31**, 4324 (1992).
9. E. P. Baldwin, J. Xu, O. Hajiseyedjavadi, *Techniques in Protein Chemistry IV*, R. Angeletti, Ed. (Academic Press, New York, 1993), pp. 499–507. All mutants were constructed in a cysteine-free pseudo–wild-type lysozyme (referred to throughout as "wt") in which Cys^{54} and Cys^{97} were replaced, respectively, with threonine and alanine.
10. X.-J. Zhang, W. A. Baase, B. W. Matthews, *Biochemistry* **30**, 2012 (1991).
11. J. H. Hurley *et al.*, *J. Mol. Biol.* **224**, 1143 (1992); S. Daoopin, T. Alber, W. A. Baase, J. A. Wozniak, B. W. Matthews, *ibid.* **221**, 647 (1991).
12. J.-L. Fauchere and V. Pliska, *Eur. J. Med. Chem.* **18**, 369 (1983).
13. L. Serrano, A. Horovitz, B. Avron, M. Bycroft, A. R. Fersht, *Biochemistry* **29**, 9343 (1990).
14. In the selection experiment (legend to Table 1) (*9*), 92 out of 106 of the functional sequences contained Val (84) or Ile (8) at position 149. Of the 30 most stable variants (estimated stability within 2.5 kcal/mol of that of wild type), only Val (25) or Ile (5) was found. Codon conversions at position 149 for this subpopulation occurred in 17 out of 30 cases.
15. For isomorphous structures of mutant T4 lysozymes that contain single surface substitutions, the rms deviations of main-chain atoms within the COOH-terminal domain are typically less than 0.11 Å (21 structures). For mutants containing single interior substitutions, rms deviations are typically less than 0.30 Å but range up to 0.44 Å (*11*).
16. The changes in position of the centers of masses (translational component) of the helices range up to 0.77 Å, while the rotational component can be described as a combination of two rotations, one about the helix axis ("roll") and one about an axis perpendicular to the helix ("tilt"), which range up to 6.7° and 6.1°, respectively.
17. Three of the variants that have Phe or Trp at position 153 (II, III, and IV) have essentially wt torsion angles (χ_1 = −81° to −91°, χ_2 = 108° to 129°). In variant V, which has the largest structural perturbations, there is a Phe at position 153 with χ_1 = −143° and χ_2 = 140°. The other four variants (I, VI, VII, and VIII) have Leu at position 153 and all four have similar conformations (χ_1 = −160° to −173°, χ_2 = 45° to 80°). Differences in side chain rotational conformations occur in only 13 out of 59 possible torsion angles or in 7 out of 33 possible side chains.
18. Met^{133} adopts a conformation that places the S$^{\delta}$ atom in the same torsion angle as defined by the C$^{\delta 2}$ atom of Leu^{133} in wild type.
19. P. Tuffery *et al.*, *J. Biomol. Struct. Dyn.* **8**, 1267 (1991); C. Lee and S. Subbiah, *J. Mol. Biol.* **217**, 373 (1991); J. Desmet *et al.*, I. Lasters, *Nature* **356**, 539 (1992); R. L. Dunbrack Jr. and M. Karplus, *J. Mol. Biol.* **230**, 543 (1993).
20. C. Wilson, L. M. Gregoret, D. A. Agard, *J. Mol. Biol.* **229**, 996 (1993).
21. N. L. Summers, W. D. Carson, M. Karplus, *ibid.* **196**, 175 (1987).
22. W. A. Lim, A. Hodel, R. T. Sauer, F. M. Richards, *Proc. Natl. Acad. Sci. U.S.A.*, in press.
23. A. M. Lesk and C. Chothia, *J. Mol. Biol.* **136**, 225 (1980); *Philos. Trans. R. Soc. London Ser. A* **317**, 345 (1986).
24. The rms backbone differences for T4 lysozyme mutant structures in seven different crystal-packing environments range from 0.24 to 0.40 Å overall and up to 0.63 Å for individual helical segments. The variants chosen have substitutions in the NH$_2$-terminal domain that would not be expected to affect the configuration of the COOH-terminal main chain residues [Ser^{44} → Glu, space group P2, one independent molecule, 1.8 Å resolution; Ser^{44} → Trp, space group P1, four independent molecules, 2.0 Å resolution; Ser^{44} → Phe, space group P2$_1$, two independent molecules, 1.9 Å resolution; M. Blaber, X.-J. Zhang, B. W. Matthews, *Science* **260**, 1637 (1993)].
25. D. Rennell and A. R. Poteete, *Virology* **143**, 280 (1985).
26. D. C. Muchmore *et al.*, *Methods Enzymol.* **177**, 44 (1989).
27. A. R. Poteete, S. Dao-pin, H. Nicholson, B. W. Matthews, *Biochemistry* **30**, 1425 (1991).
28. R. Hamlin, *Methods Enzymol.* **114**, 416 (1985).
29. D. E. Tronrud, L. F. Ten Eyck, B. W. Matthews, *Acta Crystallogr. Sect. A* **43**, 489 (1987); D. E. Tronrud, *ibid.* **48**, 912 (1992).
30. M. Matsumura and B. W. Matthews, *Science* **243**, 792 (1989).
31. International Union of Pure and Applied Chemistry–International Union of Biochemistry Commission on Biochemical Nomenclature, *J. Mol. Biol.* **52**, 4 (1970).
32. For branched side chains the torsion angle was calculated from the atom in the side chain that was closest to the position occupied by spatially

equivalent atoms in other substitutions ($C^{\gamma 2}$ of Leu^{129} and $C^{\gamma 2}$ of Ile^{149}) (*21*).

33. The T4 lysozyme gene was amplified with polymerase chain reaction (PCR) with the use of degenerate primers encoding all 20 amino acids and one stop codon (X, X, G or T, where X is A, T, G, or C) at the target sites (*9*). Three overlapping fragments bounded by the mutagenesis sites and the gene termini were generated and subsequently linked together with PCR in two steps. The full-length mutagenized gene fragment was cut with restriction enzymes and ligated into an engineered bacteriophage λ selection vector (*9*) that relied on the activity of the cloned T4 lysozyme gene to complement a defect in its own homologous lysis (R) gene (*25*). Plaque-forming phages were isolated and functional T4 lysozyme genes were excised as part of a phagemid for both protein expression and DNA sequencing (*26*). A plate assay (*27*) was used to sort the variants into rough categories of stability and activity. A total of 106 new amino acid combinations were obtained at a frequency of 10^{-2} from the screening of 25,000 phages, and a number of these were chosen for crystallographic and thermodynamic analysis. Protein preparation (*27*), thermal denaturation at pH 3 (*10*), and crystal growth (*3*) were as described. Data from x-ray measurements were collected (*28*), and structures were refined (*29*) starting with the cysteine-free wt model (*30*). No torsion angle restraints were imposed during refinement. Final models have deviations from ideal geometry less than or equal to 0.015 Å (bond lengths) and 2.1° (bond angles).

34. We thank J. H. Hurley, X.-J. Zhang, and A. R. Poteete for helpful discussions and S. Pepiot, J. Xu, and N. Gassner for help with the purification and analysis of various mutant lysozymes. Supported by a National Institutes of Health postdoctoral fellowship (GM12989) (E.P.B.) and grant (GM21967) (B.W.M.).

29 June 1993; accepted 19 October 1993

Modulation of Calmodulin Plasticity in Molecular Recognition on the Basis of X-ray Structures

William E. Meador, Anthony R. Means, Florante A. Quiocho*

Calmodulin is the primary calcium-dependent signal transducer and regulator of a wide variety of essential cellular functions. The structure of calcium-calmodulin bound to the peptide corresponding to the calmodulin-binding domain of brain calmodulin-dependent protein kinase IIα was determined to 2 angstrom resolution. A comparison to two other calcium-calmodulin structures reveals how the central helix unwinds in order to position the two domains optimally in the recognition of different target enzymes and clarifies the role of calcium in maintaining recognition-competent domain structures.

Calmodulin (CaM) exerts its role by activating more than 20 different enzymes in eukaryotic cells. Studies in solution show that the helical content of CaM is increased upon binding Ca^{2+} (*1*). The next step in the mechanism of signal transduction requires binding of Ca^{2+}-CaM to an acceptor protein. Much of what is known about such physical interactions comes from the use of synthetic peptides corresponding to the CaM-binding domains of various physiologically relevant target proteins or enzymes and also peptide drugs and toxins (*2*). Often these peptides have very little sequence similarity (Fig. 1). Calcium-CaM bound to these peptides [dissociation constant values in the nanomolar range (*2*, *3*)] has been shown especially by physical techniques to be considerably more compact than the unbound form, which indicates the extraordinary flexibility of CaM (*4*). These observations led to suggestions that in the Ca^{2+}-CaM-peptide ternary complex the two domains of Ca^{2+}-CaM interact simultaneously with opposite ends of the peptide (*2*, *4*). The x-ray structures of native Ca^{2+}-CaM show that the two domains, each containing a pair of Ca^{2+} atoms, are widely separated by a seven-turn central or linker helix with an unusually high thermal motion (*5*–*7*). The three-dimensional structure determinations of Ca^{2+}-CaM bound to synthetic peptide analogs of the CaM-binding regions of skeletal and smooth muscle myosin light chain kinase by nuclear magnetic resonance (*8*) and x-ray crystallography (*9*), respectively, have revealed that a portion of the central helix in the unbound structure uncoiled, enabling the two domains to engulf the helical target peptides. The mode of binding of the regulatory light chain seen recently in the S1 myosin crystal structure (*10*) has features that resemble those of the bound Ca^{2+}-CaM structures.

Our report focuses on the detailed structural basis for the ability of CaM to recognize the different targets and initiate signal transduction. We report the refined 2 Å structure of the complex of Ca^{2+}-CaM with the CaM-binding domain peptide (Fig. 1) of the brain CaM-dependent protein kinase IIα (CaMKII) (Fig. 2) and compare it to the 1.7 Å structure of Ca^{2+}-CaM (*7*) and the 2.4 Å structure of the complex with the different peptide from smooth muscle myosin light chain kinase (smMLCK) (*9*), which has been further refined at 2.2 Å (*11*). Whereas the smMLCK peptide is observed in its entirety in the electron density of the refined complex structure (*9*), only residues 293 to 310 of the CaMKII peptide show density and make contacts of 4 Å or less with Ca^{2+}-CaM (Figs. 2 and 3, A and B). The ordered segments define more closely the CaM-binding domain of the target enzymes within the context of the peptide fragments.

As can be seen in Figs. 2B and 3A, the ellipsoidal compact structure of Ca^{2+}-CaM bound to the CaMKII peptide bears some resemblance to that bound to the smMLCK peptide (*9*). The two domains of Ca^{2+}-CaM (identified as NH_2- and COOH-domains or lobes) wrapped around and engulfed the target peptide. The two domains approach in the central latch region (between helices II and VI) to again create a pseudo twofold symmetry and a continuous hydrophobic arc, formed from the coalescing of the wide hydrophobic patches in both domains, that apposes the hydrophobic side of the helical peptide. The NH_2- and COOH-terminal halves of the CaMKII peptide interact mainly with the COOH- and NH_2-domains of Ca^{2+}-CaM, respectively, with the exception of the consecutive basic side chains (Arg^{296}-Arg^{297}-Lys^{298}) in the NH_2-terminus, which make hydrogen bonding and salt-linking interactions with glutamate residues on both domains. Aiding maximal contact of the Ca^{2+}-CaM lobes with the target peptide, a portion of the central helix in the native Ca^{2+}-CaM structure again is pulled out into a strand (Fig. 3C), which we have referred to earlier as the "expansion joint" to underscore this unique and functionally critical region of CaM (*9*).

Consistent in part with previous general suggestions [summarized in (*2*)], a major determinant in molecular recognition appears to be the hydrophobic interactions between the shallow hydrophobic pockets in the two domains of Ca^{2+}-CaM and specific hydrophobic residues of target peptides. As can be seen in Figs. 2B and 3A, the pocket in the COOH-domain harbors Leu^{299} of the CaMKII peptide or its coun-

CaMKII peptide (residues 290 to 314)	LKKFNARRKLKGAILTTMLATRNFS
smMLCK peptide (residues 796 to 815)	ARRKWQKTGHAVRAIGRLSS

Fig. 1. Peptide segments corresponding to the CaM-binding domains of CaMKII and smMLCK used in the x-ray studies (*17*). The alignment of the peptide sequences is based primarily on an almost total identity between residues 295 to 299 of the CaMKII peptide and residues 796 to 800 of the smMLCK peptide (Fig. 3, A and B).

W. E. Meador and F. A. Quiocho, Howard Hughes Medical Institute and Departments of Biochemistry and Molecular Physiology and Biophysics, Baylor College of Medicine, Houston, TX 77030.
A. R. Means, Department of Pharmacology, Duke University Medical School, Durham, NC 27710.

*To whom correspondence should be addressed.